ESA CONTRACT REPORT

Technical Note to the European Space Agency

TN17.3: Testing the behaviour of wind retrievals with new E2S simulation options

December 2014

Michael Rennie

European Centre for Medium-Range Weather Forecasts
Europäisches Zentrum für mittelfristige Wettervorhersage
Centre européen pour les prévisions météorologiques à moyen terme

ECMWF

Series: ECMWF - ESA Contract Report

A full list of ECMWF Publications can be found on our web site under:
http://www.ecmwf.int/publications/

TN17.3

Testing the behaviour of wind retrievals with new E2S simulation options

Authors

MICHAEL RENNIE
ECMWF

CHANGE LOG

Version	Date	Comment
1.0	9 July 2014	MR: Initial attempt
1.1	6 Aug 2014	MR: finalising first draft for distribution
1.2	12 Aug 2014	MR: A few extra figures and edits following comments from Oliver Reitebuch and Thomas Kanitz
1.3	5 Dec 2014	MR: update following A. G. Straume review

Contents

1 Introduction

This technical note presents experimentation performed using the Chain-of-Processors software to assess the impact on HLOS winds (mostly L2B) of the more realistic simulation options of E2S v3.04 (released in June 2014 by Dorit Huber, DoRIT). This document is the output of work package 2830 of CCN5 (Change Request No: 5, Aeolus Level 2B/C Enhancements and Launch Extension of ESA Contract No: 4200018555/04/NL/MM Development and Production of Aeolus Wind Data Products). WP2830 regards "Extended end-to-end testing: Investigating the effect of new E2S features on L2B products". In particular it states that the following new features of E2S shall be tested:

- The simulation of Rayleigh-Brillouin scattering (i.e. pressure effect)
- ACCD read-out (vertical bin) overlap
- Rayleigh spot location imperfection
- Mie tilted fringe
- Varying ground reflectance map

Testing of these features was performed and is reported in the sections of this document.

1.1 Documents

1.1.1 Applicable documents

	Title	Ref	Ver.	Date
[AD1]	Change Request No: 5, Aeolus Level 2B/C Enhancements and Launch Extension of ESA Contract No: 4200018555/04/NL/MM Development and Production of Aeolus Wind Data Products		1.1	24/01/2014

1.1.2 Reference documents

	Title	Ref	Ver.	Date
[RD1]	Correcting winds measured with a Rayleigh Doppler lidar from pressure and temperature effects, Dabas et al.	Tellus A, 60(2), 206–215, 2008		2008
[RD2]	E2S Issue 3/04 Software Release Note	ADM-RN-52-2890	3/04	Jun 13 2014
[RD3]	E2S modelling	AE-TN-DLR-E2S-001	1.3	31/7/2012
[RD4]	End-to-end testing of the continuous mode L2B processor	AE-TN-ECMWF-GS-153	3.1	19/3/2014
[RD5]	ADM-Aeolus level-2B algorithm theoretical baseline document	AE-TN-ECMWF-L2BP-0024	2.4	Dec 2012
[RD6]	B. Witschas, 'Analytical model for Rayleigh–Brillouin line shapes in air' ,	APPLIED OPTICS / Vol. 50, No. 3 / 20 January 2011		2011
[RD7]	On the kinetic model description of Rayleigh-Brillouin scattering from molecular gases,	G. Tenti, C. Boley, and R. Desai, Can. J. Phys. 52, 285–290		1974

1.2 Acronyms

ACCD	Accumulation Charge Coupled Device
AOCS	Attitude and Orbit Control System
ATBD	Algorithm Theoretical Baseline document
BM	Burst mode
BRC	Basic Repeat Cycle
CM	Continuous mode
CoP	Chain-of-processors software
DA	Data assimilation
DCMZ	Dark current in memory zone
DEM	Digital Elevation Model
DWL	Doppler Wind Lidar
ECMWF	European Centre for Medium-Range Weather Forecasts
EGM	Earth Gravitational Model
ESTEC	European Space Research and Technology Centre (part of ESA)
HLOS	Horizontal Line Of Sight
IODD	Processor Input/Output Data Definitions Interface Control Document
KNMI	Royal Netherlands Meteorological Institute
LOS	Line of sight
L1B	Level-1B
L2B	Level-2B
L2Bp	L2B processor
N/A	Not applicable
NWP	Numerical weather prediction
QC	Quality control
RB	Rayleigh-Brillouin
RMA	Reference model atmosphere
RR	Rayleigh response
RRC	Rayleigh response calibration
SNR	Signal to noise ratio
SRD	System requirements document
TBD	To be determined
TN	Technical note
VHAMP	Vertical and Horizontal Aeolus Measurement Positioning
WGS	World Geodetic System
WP	Work package
XML	Extensible Markup Language

ZWC   Zero wind correction

2   E2S simulation of the Rayleigh-Brillouin backscatter spectrum

An option to simulate the effect of pressure on the atmospheric molecular backscatter is available in E2S v3.04. This effect is known as Brillouin scattering, in which the atmospheric backscatter spectrum shows dependence upon pressure. Earlier versions of the E2S simulated the effect of temperature only (i.e. Rayleigh scattering which has a Gaussian spectrum). The combined temperature and pressure effect is Rayleigh-Brillouin scattering.

Brillouin scattering is an interaction between an electromagnetic wave and crystalline lattice waves which alter the refractive index. In the atmosphere, these waves occur as mass oscillation (acoustic) modes which become more important as the pressure increases. Rayleigh scattering, too, can be considered to be due to fluctuation in the density, composition and orientation of molecules, and hence of refraction index, in small volumes of matter (particularly in gases or liquids). The difference is that Rayleigh scattering considers only random and incoherent thermal fluctuations, in contrast with the correlated, periodic fluctuations (phonons) that cause the Brillouin scattering. The Rayleigh-Brillouin effect on the backscattered laser light is now modelled in the E2S using an analytical model, described in [RD6]. Figure 1 shows an example comparison of the Rayleigh and Rayleigh-Brillouin scattering spectrum in the atmosphere (lower troposphere) as simulated by the E2S.
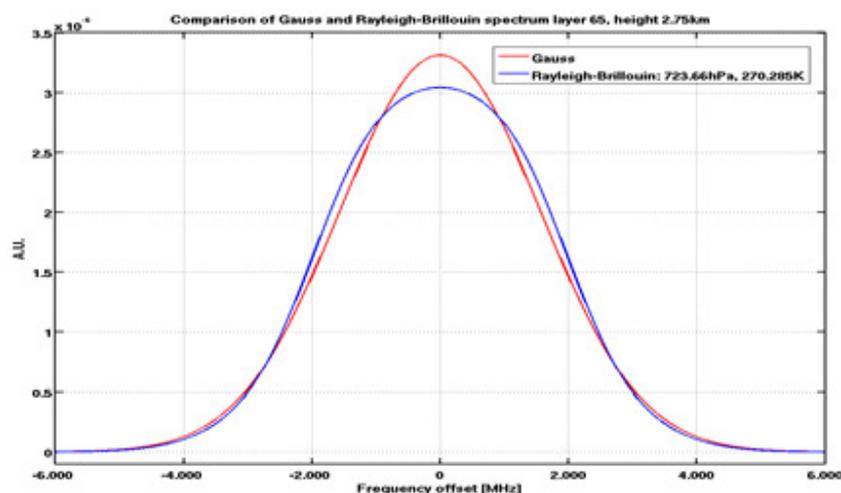

Figure 1.   Comparison of a Rayleigh scattering spectrum (red) and Rayleigh-Brillouin scattering (blue) spectrum from the E2S for T=270K and P=723 hPa. Courtesy of Dorit Huber.

The use of this new E2S feature is controlled via the E2S settings file:

`atmosphereProfileParameters.xml`

in particular it can be switched on by setting:

`<rayleighBrillouinFlag>true</rayleighBrillouinFlag>`

Tests were performed with and without the Brillouin scattering in the E2S. The aim was to confirm that simulating this effect leads to a noticeable pressure dependence of the errors in Rayleigh HLOS wind. Also that the L2B processor can correctly remove this pressure effect when using an appropriate

Rayleigh calibration (AUX_RBC_L2) input file and a priori pressure information (AUX_MET_L2).

Tests were run at ECMWF using the Chain-of-Processors (CoP) software (see Figure 2 for an impression of how the CoP testing works).
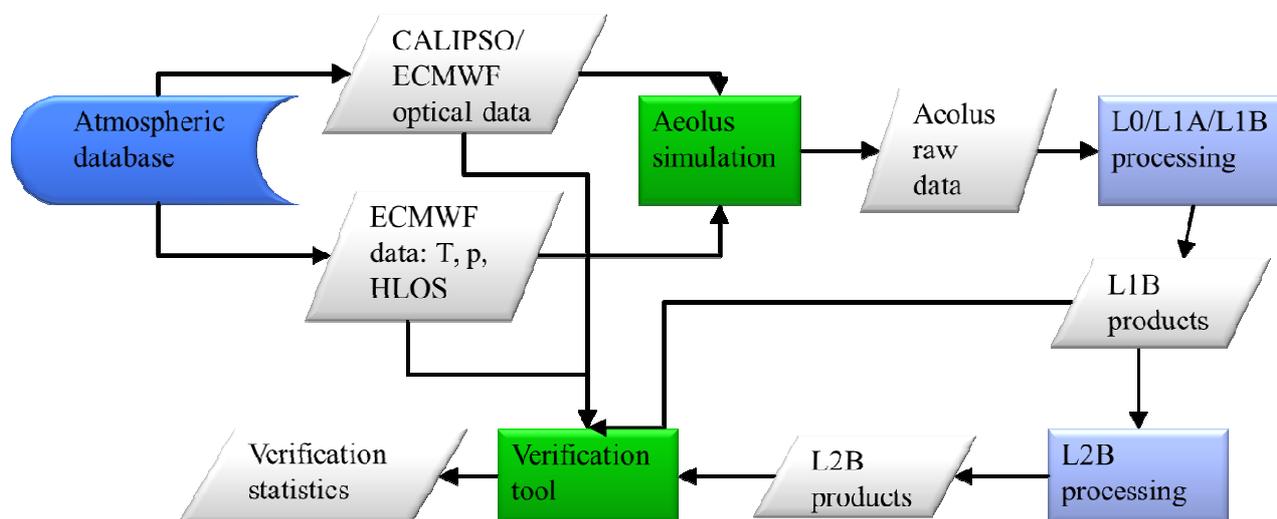

Figure 2. The steps involved in running CoP testing and verification of the wind results.

Some updates to the CoP software were required (by Jos de Kloe (KNMI) and by myself) for new software versions i.e. E2S v3.04, L1Bp v6.03 and L2Bp v2.10.

The tests involve:

1. Switching "on" the RB effect in E2S

2. Running the CoP scenario up to L2B results with appropriate calibration files. Experiments were done using an AUX_RBC_L2 file which includes Rayleigh responses which vary correctly as a function of pressure, and with an AUX_RBC_L2 which does not account for changes with pressure (i.e. as if p=0 hPa). Alain Dabas (Météo-France) provided two such AUX_RBC_L2 files for testing

3. Running the verification statistics (IDL tool at ECMWF). Interpreting the verification statistics for the L2B wind results (see [RD4] for a description of the error statistics calculations done at ECMWF). Confirming that the L2B processing with the "correct" AUX_RBC_L2 improves the wind results relative to the AUX_RBC_L2 which does not account for pressure.

The Brillouin scattering effect should be largest at the highest atmospheric pressures i.e. towards the surface. According to [RD1], not accounting for the pressure effect can lead to LOS wind errors of the order several m/s near the surface, so this is a large source of systematic error if left uncorrected.

As discussed in section 2.3.2 below, the AUX_RBC_L2 correction for Brillouin scattering is based on the modelling of Rayleigh-Brillouin scattering effects using the so-called Tenti S6 model ([RD7]). This model is not identical to the model described in [RD6], which is used to simulate the scattering by the E2S. The model from [RD6] has been fitted to closely match the [RD6] model. Comparisons of

simulated spectra using both models have shown that the difference between the two is on the sub-percent level ([RD6]). This is expected to be low enough to not cause any significant error contributions when applying the AUX_RBC_L2 correction.

2.1 AUX_RBC_L2 files and RB correction

The applied AUX_RBC_L2 files provides a look-up table of Rayleigh response (RR vs. frequency) curves for the following combinations of temperature and pressure (i.e. RR curves for each of these combinations):

Tgrid=[170 , 180 , 190 , 200 , 210 , 220 , 230 , 240 , 250 , 260 , 270 , 280 , 290 , 300 , 310 , 320 , 330] in K

Pgrid=[10 , 110 , 210 , 310 , 410 , 510 , 610 , 710 , 810 , 910 , 1010] in hPa

The L2B processor has been developed to make use of the AUX_RBC temperature and pressure correction of the Rayleigh responses, but the pressure correction part has not yet been verified since the E2S has only been able to simulate Brillouin scattering with E2S v3.04. In the L2B processor subroutine CORRECTION (part of `Tentispectrum.F90`), the RB correction finds the RR curve for the p and T combination (in the AUX_RBC file) closest to that suggested by the AUX_MET_12 at the observation geolocation. The nearest RR value to the observed RR gives the frequency and hence Doppler shift of the observation. See [RD5] for a complete description of the "ILIAD" correction. These tests will confirm if this grid has enough sampling for accurate interpolation.

2.2 Test case

The chosen CoP test scenario (called "Test_TN3_1_0005_more_segments", created for this test) is very simple: there is no cloud or aerosol (i.e. clear atmosphere) so that Rayleigh winds without Mie signal contamination are available. It includes a range of HLOS values [-50.0,-20.0,0.0,20.0,50.0] m/s so that the calibration response curves are sampled over many frequencies (not just near the Rayleigh transmission cross-point). There are 80 BRCs (so each wind value is sampled 16 times) and the HLOS wind is set to be constant for each BRC on all height ranges. All sources of random errors are switched off in the E2S so that the systematic effect of the pressure correction (or lack of) is clearly seen. The atmospheric profiles for temperature and pressure are fixed in the horizontal dimension to the RMA_profile_for the subarctic_winter.

2.3 Verification of the pressure effect on L2B Rayleigh-clear HLOS winds and its correction by the AUX_RBC file

2.3.1 L2B wind retrieval without pressure correction

Figure 3 shows the E2S input HLOS wind (i.e. true HLOS) as a function of the satellite along-ground track distance and altitude (above Earth geoid) for the scenario. The 'classic' grouping in the L2B processor was chosen, so that one wind observation is based on the measurements available in one BRC (for a particular range gate).
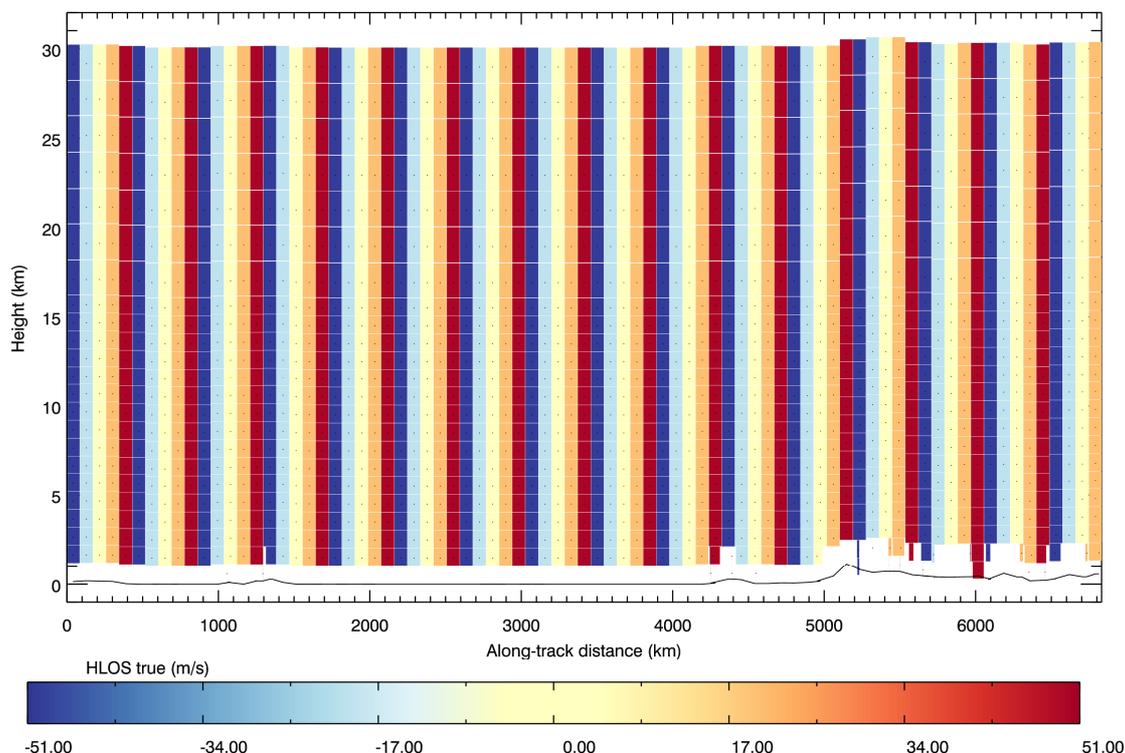
Figure 3. The true HLOS winds shown as a "curtain" along the ground track of the satellite. Colours indicate the values of HLOS wind (m/s). The rectangles indicate the spatial extent of the observations i.e. size of range-bin and horizontal extent of the measurements used in the observation.

Figure 4 shows the corresponding HLOS error on the same grid as Figure 3 for the Rayleigh-clear L2B wind results when a correction of the pressure modification of the Rayleigh Response has not been taken into account because the AUX_RBC_L2 files did not include such a variation: the error is defined as (*true HLOS - L2B HLOS*). It can be seen that the magnitude of the errors increase towards the surface (i.e. at higher pressure). The errors are not visible with this colour-scale above 11 km. The size and sign of the errors depend on the true HLOS value: they are negative (blue) for -50 m/s HLOS winds and positive (red) for +50 m/s, for HLOS winds in between the errors are smaller.
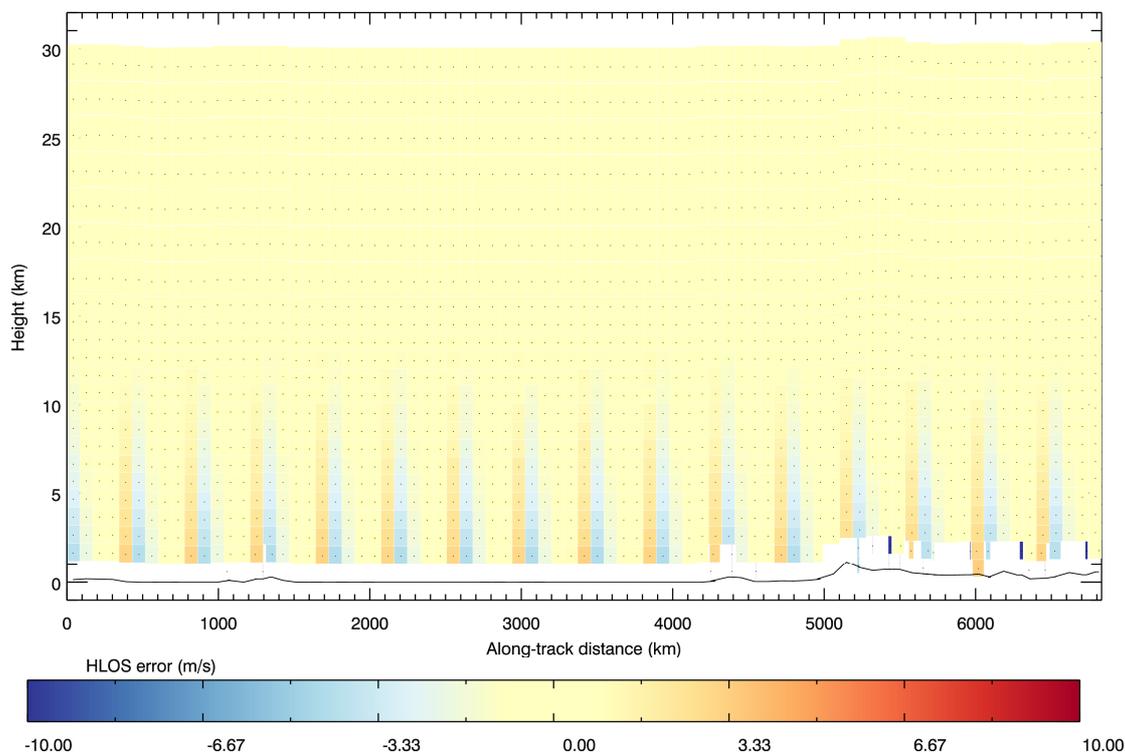
Figure 4. The HLOS error (true minus L2 obs) in the same format as Figure 3.

Figure 5 shows the error dependence upon pressure; clearly there are systematic effects. In fact there is a roughly linear increase in bias towards high pressures, the gradient of which depends on true HLOS value (each "spoke" is for a different HLOS wind). The systematic error increase with pressure reaches around -4 m/s near the surface (~900 hPa) i.e. the bottom "spoke" of results which corresponds to the -50 m/s HLOS wind as truth. The bias reaches +3 m/s for +50 m/s HLOS wind near the surface (top "spoke" of results). The asymmetry relative to 0 m/s HLOS true wind is because the cross-point of the transmission filters (A and B) for the Rayleigh channel is not located at 0 m/s HLOS, but at some positive value.

The "spokes" between the two extremes are for intermediate values of true HLOS winds. The biases become small at pressures less than 100 hPa (which is roughly 15 km altitude). Remaining biases at this level are believed to be due to the DCMZ effect described in [RD4].
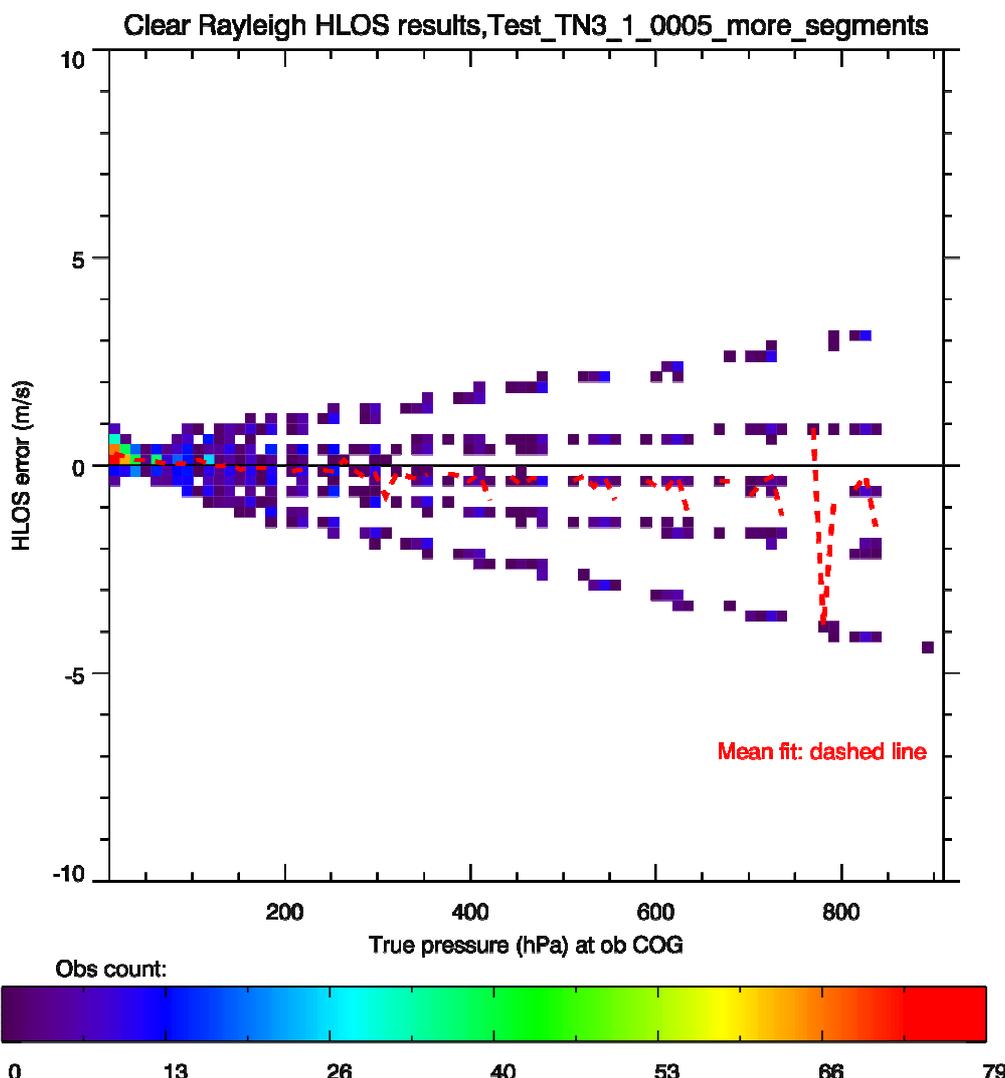
Figure 5. Density plot of the dependence of HLOS error on the pressure for the Rayleigh-clear L2B winds.

The magnitude of the systematic errors agree with [RD1]. It is important to correct the HLOS dependence on pressure for Aeolus Rayleigh winds, since this level of bias would severely limit the impact of the observations in NWP.

2.3.2 L2B wind retrieval applying pressure correction

With the "correct" AUX_RBC_L2 calibration file i.e. one which does account for the modification of the response with pressure (when used in combination with E2S scenario that simulates RB scattering), then we get Figure 6 (which can be compared to Figure 5). As hoped for, the biases are small and there is no clear dependence of the HLOS error upon pressure (again residual biases at higher levels are due to the DCMZ effect). Therefore this confirms that the RB correction scheme in the L2B processing works. This is the first time that the L2Bp correction scheme has been confirmed to work correctly for the pressure effect of the RB scattering.
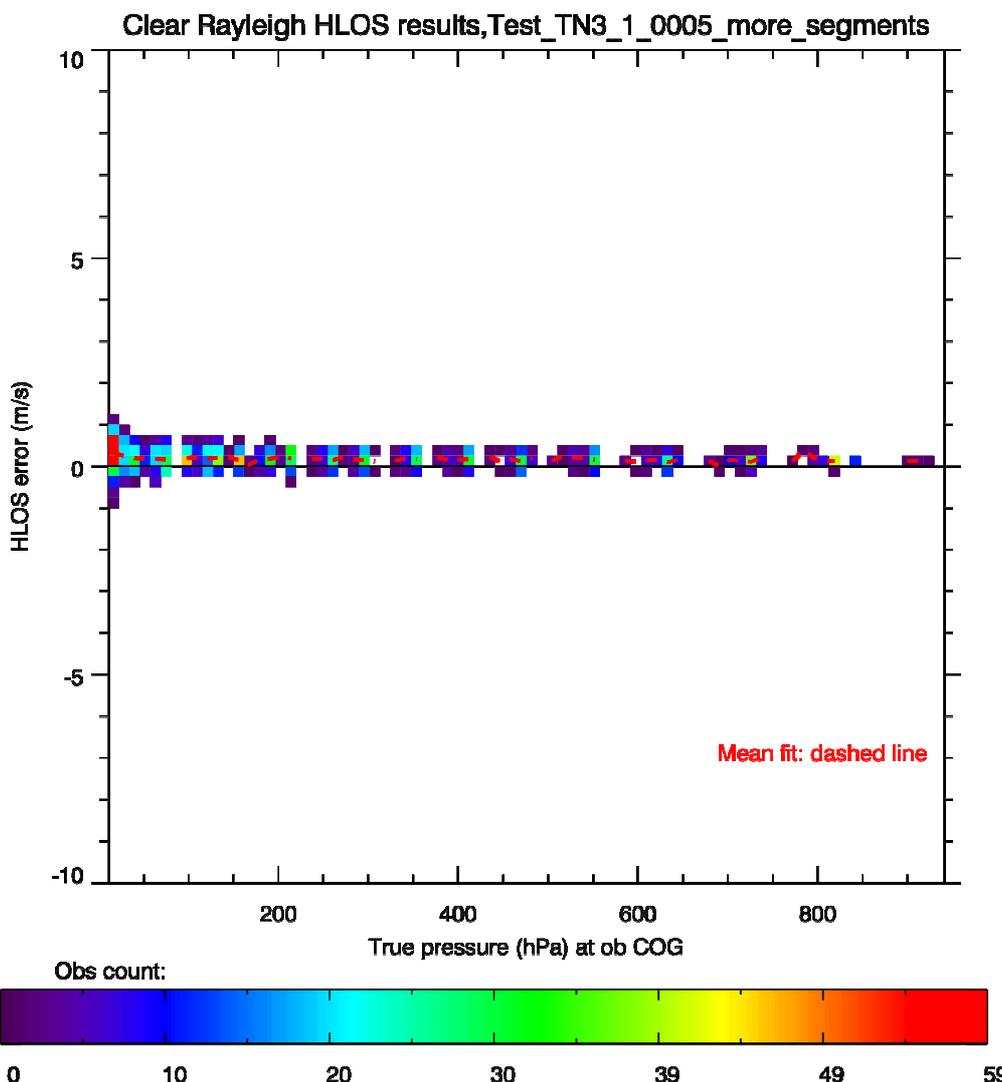
Figure 6. The same as Figure 5, but using the correct AUX_RBC_L2 in the L2Bp which accounts for pressure.

It appears that the pressure grid in the AUX_RBC_L2 (with only 11 values) is sampled regularly enough to give an accurate correction of the pressure effect.

The generation of useful AUX_RBC_L2 calibration files depends on an accurate model of the Rayleigh-Brillouin spectrum; currently it uses the Tenti-S6 model. In this test case the AUX_RBC generation model matches the E2S simulation (which is done using a simpler parameterized version of the Tenti-S6 model as developed by B. Witschas, see [RD6]) and hence these results are perhaps too optimistic since the real atmospheric spectrum may differ to some extent, although recent experimentation at University of Amsterdam suggests the Tenti-S6 model is accurate enough. The results confirm that the Witschas parameterized model is sufficiently close to the Tenti-S6 model for this correction to work.

In this test case the a priori pressure estimate perfectly matched the E2S input pressure, but in reality the AUX_MET_12 (i.e. ECMWF short-range forecast) will have errors in the pressure as a function of altitude. Surface pressure errors for particularly poor forecasts (e.g. tropical cyclones central pressure) can have errors of around 30hPa in the background forecast (which can be improved

with higher model resolution). [RD1] states that the typical sensitivity of the pressure correction to errors in pressure is ~0.003 (m/s)/hPa LOS (for a RR on the more extreme end of the response), so the error in HLOS for the 30 hPa (extreme surface pressure error) would be around 0.15 m/s HLOS, which is a relatively small systematic error and so is unlikely to concern NWP users, especially since ECMWF surface pressure errors are more typically several hPa in extra-tropical conditions.

The L1B processor does not correct for RB effects (this is one reason for the further processing to L2B before use). The L1B Rayleigh HLOS wind error statistics as a function of temperature (Figure 7) and pressure (Figure 8) are shown below. This suggests that there is some cancellation of the biases from the two effects (i.e. temperature and pressure) near the surface (when compared to Figure 5), leaving smaller biases in the L1B winds than seen for the pressure effect (in L2B winds) alone. The biases are still up to -4 m/s with the combination of HLOS=-50 m/s, temperature=-55 K and pressure=300 hPa, which is unacceptable for NWP.
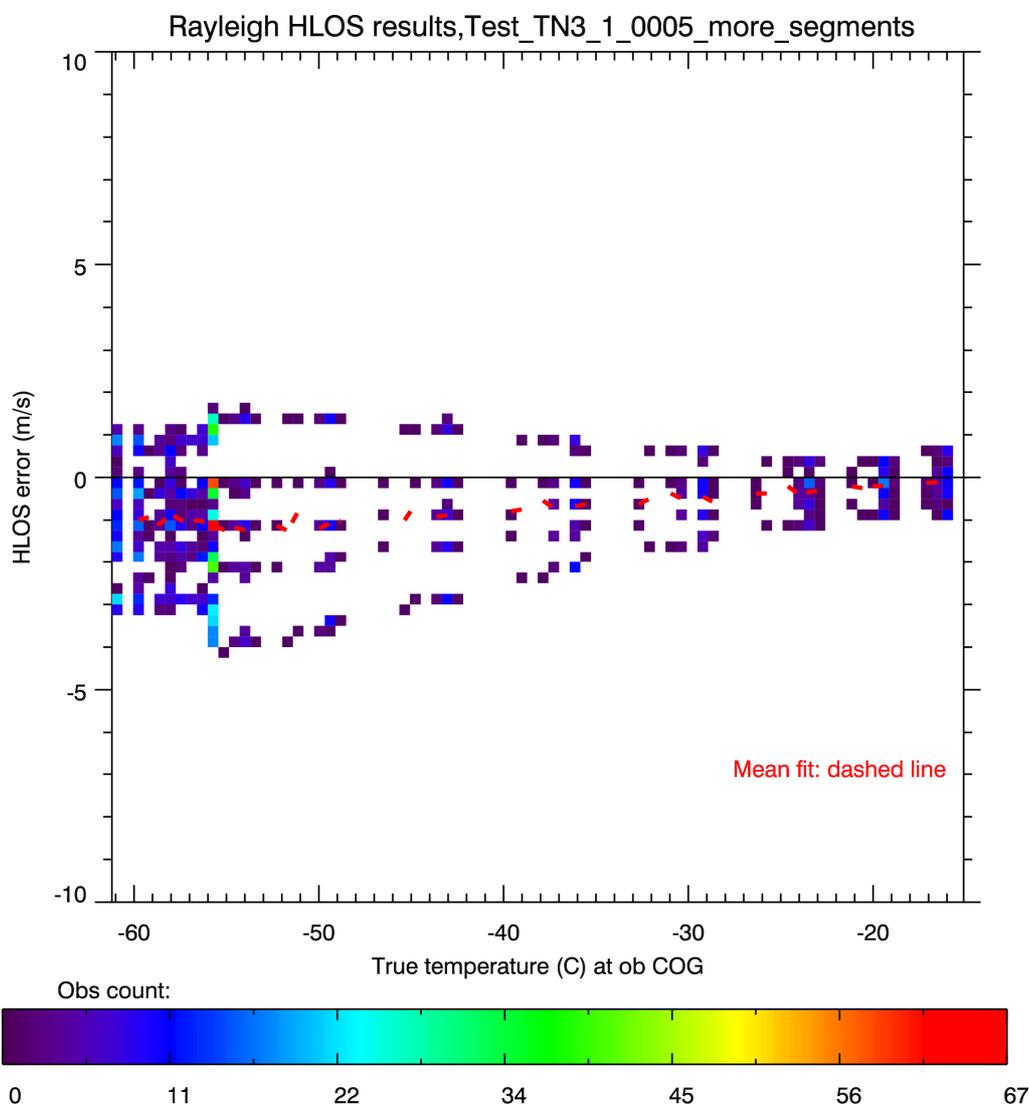

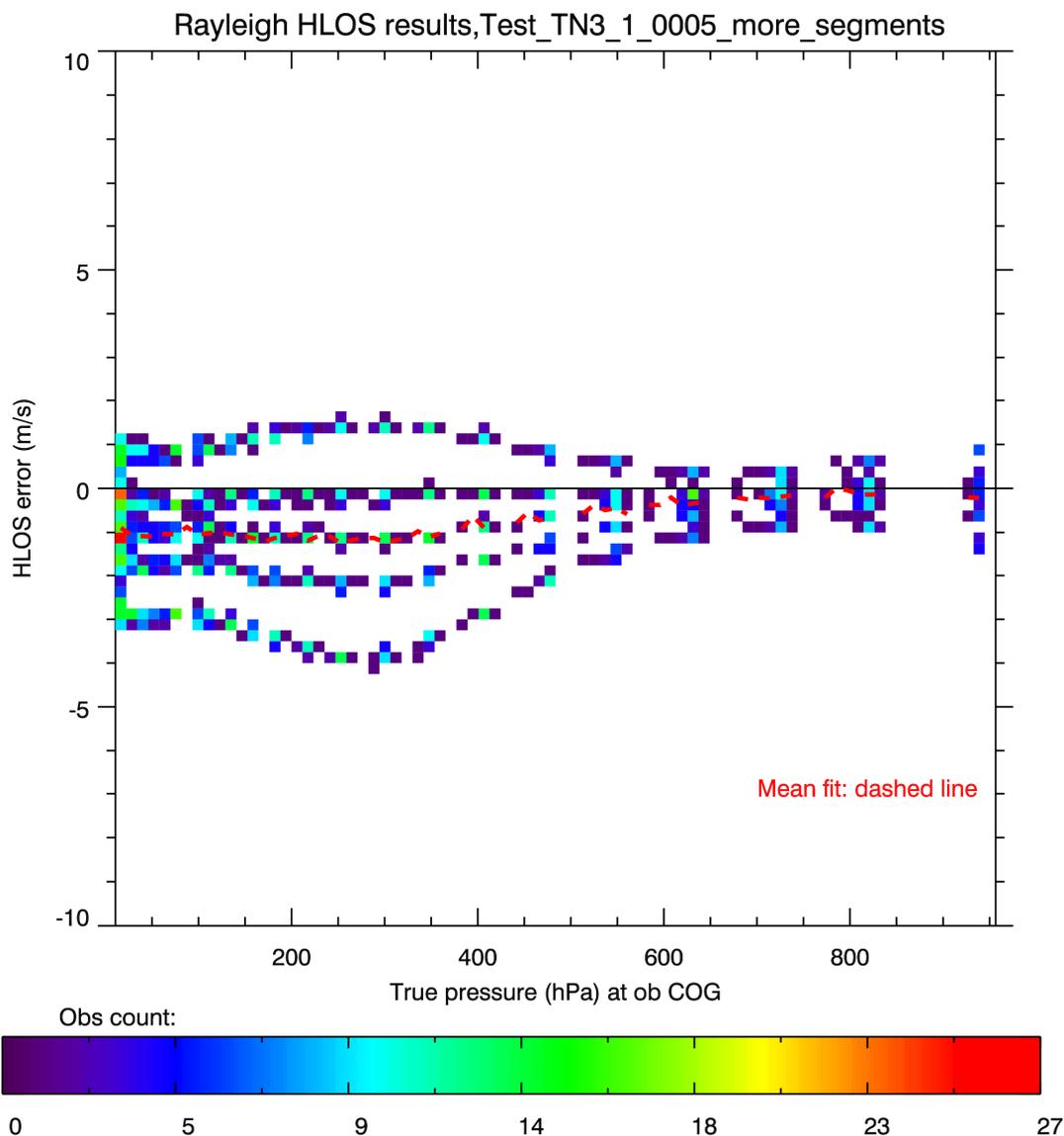Figure 7. Dependence of L1B Rayleigh HLOS wind error upon temperature.

Figure 8. Dependence of L1B Rayleigh HLOS wind error upon pressure.

In conclusion, the RB scattering simulation in E2S can be accurately corrected in the L2Bp when used with the appropriate AUX_RBC_L2 calibration file, assuming that the Tenti S6 model is an accurate parameterization of the true RB scattering in the atmosphere.

3 Vertical-bin-overlap for Mie and Rayleigh

E2S v3.04 includes the optional simulation of vertical-bin-overlap. According to [RD2] and [RD3] the vertical-bin-overlap effect is a result of the data readout procedure of the ACCD. Readout of the ACCD and data acquisition is performed in parallel. This leads to a smearing effect of signal on neighbouring height bins.

The read out process of the ACCD columns can be modeled in two alternative ways in the E2S.

The simple default model assumes that the readout requires no time and can be performed in the instrument instantly (this has been used in the simulation for previous versions of E2S). If selected in the input parameters file, a different readout process is simulated. It assumes a read out duration where the charge on the ACCD image zone is pushed downwards row per row into the transfer row. During this readout phase, atmospheric signal is continuously acquired on the ACCD. Going from one range bin to the next, this readout process causes what is referred to as vertical-bin-overlap; basically some signal from bin i+1 is read as bin i and some signal from bin i is read as bin i+1. [RD3] provides a description of how the new readout method in implemented in E2S v3.04.

The effect of vertical-bin-overlap on the L2B winds is investigated with a Chain-of-Processors test scenario in which the E2S `satelliteParameters.xml` file has been modified to switch on the vertical-bin-overlap effect i.e.

```
<verticalBinOverlap>1</verticalBinOverlap>
```
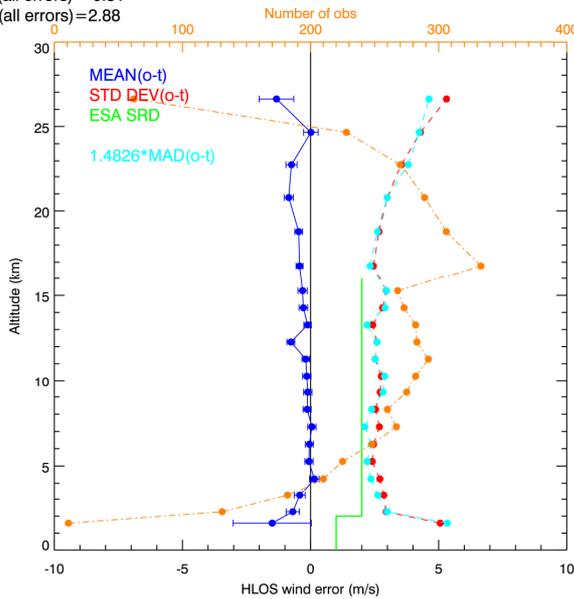
3.1 Test case

The chosen Chain-of-Processors test case is the 1st half-orbit CALIPSO scenario from the KNMI database. This should provide a sufficiently large sample of wind results for any effect of vertical-bin-overlap to become apparent. It has reasonably realistic variability of meteorological inputs. The scenario was run twice, once with the vertical-bin-overlap effect "on" and once "off". Since the "normal" sources of random error in the E2S were switched "on" in both the experiment and control (i.e. E2S default settings), one can expect that additional random differences in wind results other than the effects of vertical-bin-overlap will exist. The Rayleigh channels spots and Mie Fizeau fringe on the ACCD are set to the E2S default values i.e. perfectly aligned. This is important since the imperfections interact with the vertical-bin-overlap (as will be investigated in sections 4 and 5).

The L2B processor was set to "advanced" grouping, with 70 km horizontal accumulation length for the Rayleigh and 40 km for the Mie (the averaging length influences the level of noise seen in the L2B wind results). These are currently thought to be the best settings, in terms of use for global NWP (at ECMWF).
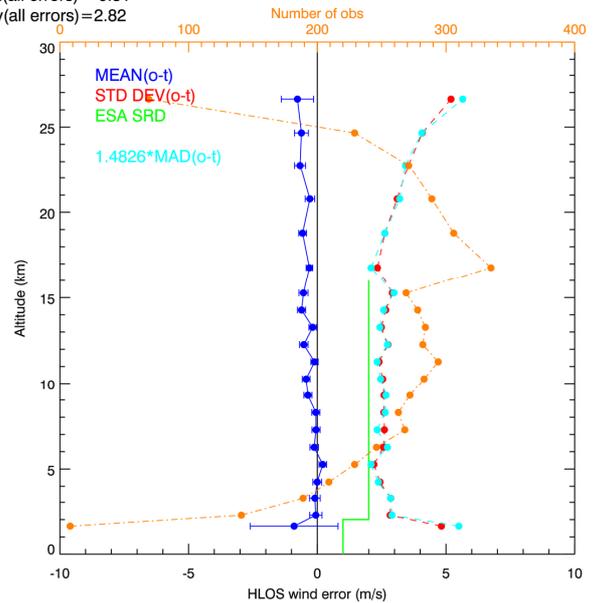
3.2 Results

Figure 9 and Figure 10 show the error statistics for Rayleigh-clear and Mie-cloudy L2B winds respectively. The dark blue line is the mean error (i.e. bias), red is the standard deviation of error (and light blue is a robust statistic for random error, for comparison to standard deviation) and orange is the number of results per level. In each figure the vertical-bin-overlap "on" case is shown in (a) and the vertical-bin-overlap "off" is shown in (b). Note that some quality control (QC) of the error statistics is performed using the L2B error estimates (i.e. the calculated error estimates with each wind result): wind results are rejected for the Rayleigh channel if predicted standard error > 5 m/s and if > 3 m/s for the Mie. This QC has been tuned to exclude outliers which would damage the non-robust metrics like mean and standard deviation (the fact that the robust statistic, median absolute deviation (MAD), agrees with standard deviation indicates that outliers are being QC'ed).

Figure 9. Error statistics for Rayleigh-clear L2B HLOS with vertical bin-overlap in a) and without vertical bin-overlap in b)
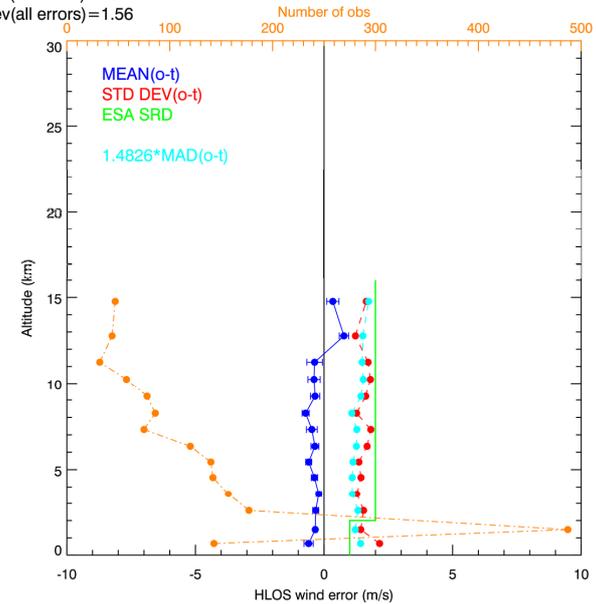

Figure 10. Error statistics for Mie-cloudy L2B HLOS with bin-overlap in a) and without bin-overlap in b)

From Figure 9 and Figure 10 the errors statistics are very similar with and without vertical-bin-overlap. That is, vertical-bin-overlap per se has little effect on the wind results (see section 4 for what happens when combined with "imperfections" in the interferometers). However the slightly larger error standard deviations with vertical-bin-overlap "on" can be attributed to this effect. Random errors

(standard deviation) are larger with vertical-bin-overlap by 2% for the Rayleigh and 7% for the Mie. This is a relatively small increase in error i.e. not too much to be concerned about from a NWP user perspective. N.B. that the negative bias of ~-0.5 m/s for the Mie channel is thought to be an issue with the MRC file provided by the L1B team (a clean version for use with L1Bp v6.03).

Vertical-bin-overlap effectively leads to a smearing of wind information over two range-bins, which would mean that the retrieved winds disagree more with "point" winds which are used as truth in this verification. This may explain the increase in standard deviation. With no vertical wind shear, there should be no increase in standard deviation and with increased vertical wind shear the errors would increase.

It would be interesting to see if the vertical-bin-overlap influences the vertical correlation of the wind errors, since we might expect it to increase them due to the lack of independence between adjacent range gates. Unfortunately it is not a simple task to calculate vertical correlation of error from such scenarios due to the occasional missing data values which are difficult to deal with when calculating covariance matrices. By manually inspecting cross-sectional views of HLOS errors for the two cases there was no obvious correlation of the errors (although it's not clear how obvious this could be). Correlated errors can be an issue for NWP use of the data (if not correctly specified in the observation error covariance matrix used in data assimilation).

In summary, it would appear that vertical-bin-overlap per se is not a great issue for the quality of atmospheric winds from Aeolus, however in the next sections, it is apparent that the effect interacts with spectrometer imperfections to become more of an issue.

4   Rayleigh Spot Location Imperfection

According to [RD2], Rayleigh Spot Location Imperfection can be simulated in the E2S v3.04. It allows the user to specify the centre position of the beam spots A and B upon the ACCD. Effects of a vertical miss-alignment of the spot centres will interact with the vertical-bin-overlap simulation (section 3), thus affecting the Rayleigh wind results.

To test this effect we need some sensible estimates of possible spot miss-alignments. Oliver Reitebuch (DLR) suggested the following:

"We have no indication about realistic settings for the spot locations from Astrium (it seems that they still have to perform this measurement) but we can use the numbers from the A2D (airborne demonstrator) – and hope this is a worst case. But the effect was observed by Astrium in the pre-development phase (10 years ago). The miss-alignments are only relevant in the vertical direction of the ACCD.

The difference in spot position is a maximum of 0.5 pixel between direct and reflected for the A2D. So maybe a value of 0.3 pixel is more realistic for ALADIN. So I changed the values of direct/reflected path vertical position 8.5+-0.15 accordingly. The settings for testing are therefore:"

```
<beamSpotCentrePixelXDirectChannel unit="pixels">8.35</beamSpotCentrePixelXDirectChannel>
<beamSpotCentrePixelYDirectChannel unit="pixels">4.5</beamSpotCentrePixelYDirectChannel>
<beamSpotCentrePixelXReflectedChannel unit="pixels">8.65</beamSpotCentrePixelXReflectedChannel>
<beamSpotCentrePixelYReflectedChannel unit="pixels">12.5</beamSpotCentrePixelYReflectedChannel>
```

An example of what a Rayleigh spot location imperfection looks like on the ACCD is shown in Figure 11 courtesy of Dorit Huber (taken from L1B PM31 slides). This is a rather more extreme spot shift, with settings of:

```
<beamSpotCentrePixelXDirectChannel unit="pixels"> 7.5 </beamSpotCentrePixelXDirectChannel>
<beamSpotCentrePixelYDirectChannel unit="pixels"> 4.2 </beamSpotCentrePixelYDirectChannel>
<beamSpotCentrePixelXReflectedChannel unit="pixels"> 9.0 </beamSpotCentrePixelXReflectedChannel>
<beamSpotCentrePixelYReflectedChannel unit="pixels"> 12.5 </beamSpotCentrePixelYReflectedChannel>
```
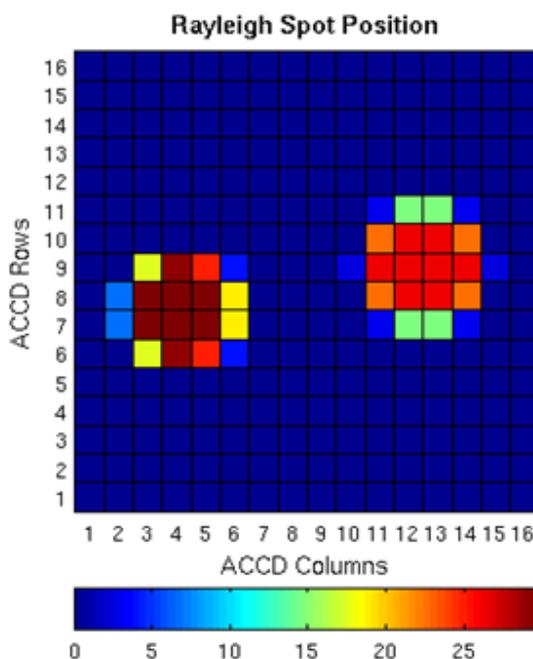

Figure 11. Rayleigh spot imperfection example. Note this is more extreme than Oliver's suggested misalignment.

4.1 Test cases

The same test case as in the section 3 has been used i.e. the 1ˢᵗ CALIPSO half-orbit case. The difference was that in the E2S settings the beam spot centres are shifted as suggested by Oliver in the `lidarInstrumentRayleighParameters.xml` file which is used by the E2S.

It was also decided to run a simpler scenario to help clarify the impact, in particular the same one as used in section 2 was used, but with the E2S simulation of vertical-bin-overlap "on" and including the above chosen Rayleigh spot imperfections (and also with "perfect" spot alignment for comparison). Remember this simpler test case has no vertical gradient in wind and random error source "off" in the E2S.

4.2 Results

Figure 12 shows the Rayleigh-clear L2B error statistics for the "realistic" case. This can be compared to Figure 9 a), i.e. the case where the Rayleigh spots are perfectly aligned. The main difference in the statistics is that the bias has changed; the standard deviation remains very similar. The bias has gone from -0.31 m/s to +0.38 m/s. This was checked to be a mostly consistent shift for different HLOS values. This +0.69 m/s HLOS bias shift is large (by NWP impact standards), showing that HLOS bias is very sensitive to the imperfect Rayleigh spot vertical alignment (given the relatively small vertical shift in the spots).
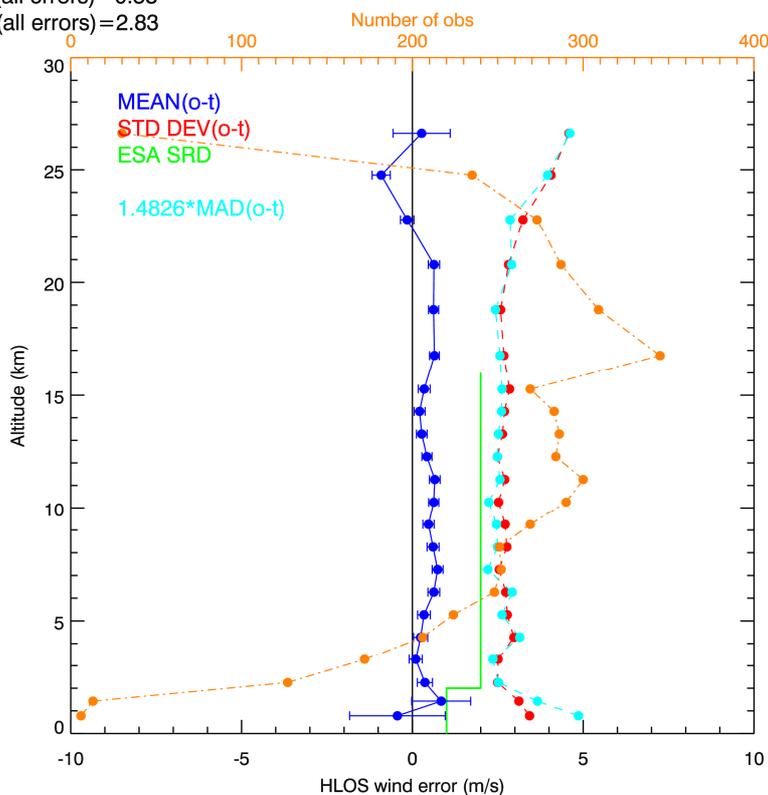
Figure 12 Error statistics for Rayleigh-clear L2B HLOS with vertical bin-overlap combined with an imperfect vertical alignment of the Rayleigh spots on the ACCD.

Figure 13 shows the effect on the much simpler test case (as discussed in previous section) of the vertical miss-alignment of the Rayleigh channel: a) is with "perfect" alignment and b) is with the vertical spot miss-alignment suggested by DLR. There is a clear shift in the bias (dark blue line) due to the spot miss-alignment by about +0.7 m/s HLOS, which is a similar value to the more realistic CALIPSO test case shown in Figure 12. Note that the bias exists in spite of the wind being constant in the vertical. This level of bias is a concern for NWP impact. Note that standard deviations are very small in Figure 13 because the E2S noise sources are switched off.
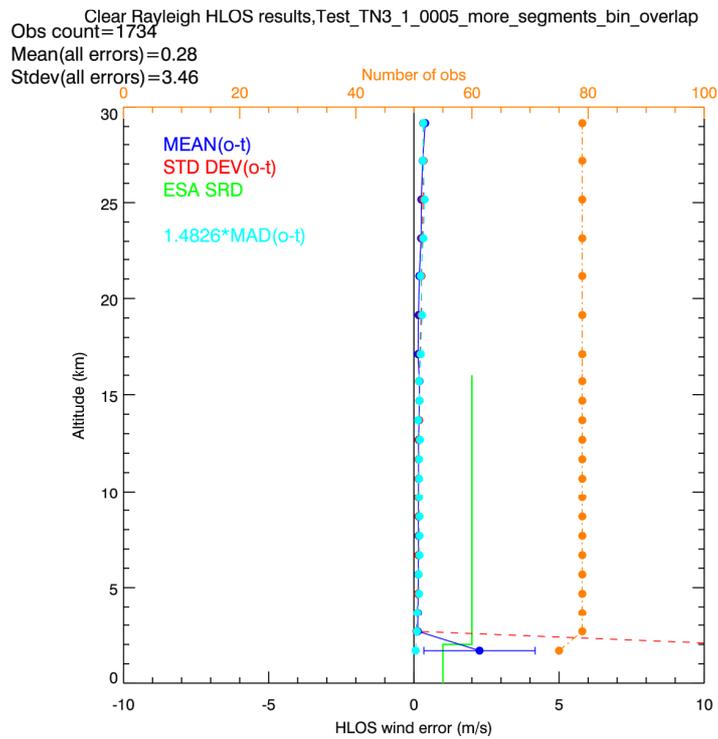
The source of the bias due to the vertical spot miss-alignment is thought to be through the following process: Vertically shifting a Rayleigh spot on the ACCD interacts with the readout process such that the signal ascribed to range bin i is contaminated more by the signal of an adjacent range bin (i+1) than if it was centred i.e. **effectively meaning a height assignment error for the shifted spot**. When combined with vertical gradients in backscatter in the atmosphere (due to density changes for the molecular backscatter) this means that the signal level (number of photons) for the shifted spot is changed relative to the other spot. For example, if the Rayleigh response with perfectly aligned spots is RR=(A-B)/(A+B), this becomes RR'=(cA-B)/(cA+B) if one spot is miss-aligned relative to the other. Therefore the Rayleigh response is altered, which leads to a HLOS bias. It seems to be a fairly consistent change due to the exponential density change in the atmosphere with height. The effect of vertical gradients of wind seems to be of less importance, given that a similar bias was reported for the

case with normal vertical wind variability (CALIPSO 1st half-orbit, Figure 12).

It is unclear if performing the RRC with the same spot imperfection will cancel out this bias for the L1B processor (N.B. the calibration used in the test cases here were based on E2S simulation with perfect alignment of the Rayleigh spots). Effectively the wind results depend on atmospheric density gradient as well. The RRC will be valid for specific bin sizes (those chosen at 6-16 km altitude).
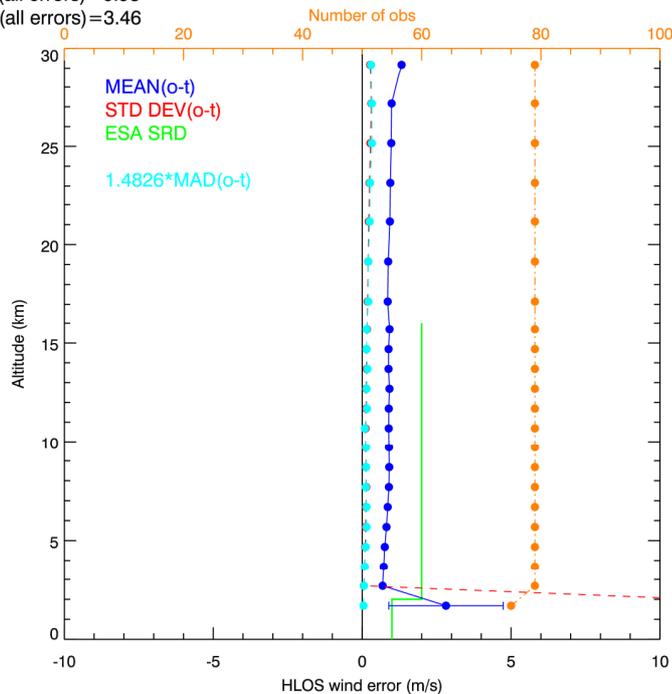
However it is clear that this cannot be accounted for with the current L2B processor calibration strategy, i.e. AUX_RBC generation. This relies on the simulation of the RRC based on knowledge of the A and B transmission functions and atmospheric backscatter spectrum. But it assumes that the A and B filters are both filtering the **same** atmospheric backscatter spectrum, however if the A and B filters are sampling the range-bins differently due to the spot imperfection then the signal levels will be different (i.e. different peaks of spectra); at present the AUX_RBC generation assumes the same spectrum is integrated by both transmission functions.

The level of Rayleigh spot alignment needs to be assessed for ALADIN to decide whether this could be a problem, and some strategy on how to deal with it needs consideration. It should also be further noted that Rayleigh spot misalignments may happen during launch or during mission lifetime due to vibration, outgassing or other degradation mechanisms w.r.t. the on-ground alignment.

Figure 13. **L2B Rayleigh-clear error statistics with vertical-bin-overlap a) with perfect Rayleigh spot alignment and b) with imperfect Rayleigh spot alignment.**

5 Mie Tilted Fringe

According to [RD2], prior to E2S v3.04 a perfectly aligned Mie fringe (fringe parallel to ACCD columns) was simulated, and only a single ACCD row was required for simulation. Measurements of the real instrument showed that the fringe is not perfectly aligned vertically with the ACCD, thus the E2S had to be modified to simulate 16 ACCD rows to allow representation of vertical-bin-overlap. Furthermore, a tilt of the fringe can now be specified in the `lidarInstrumentMieParameters.xml` file, for example:

```
<tiltedFringe>1</tiltedFringe>
<List_of_Row_Peak_Shifts count="16">
    <Row_Peak_Shift>0.0</Row_Peak_Shift>
    <Row_Peak_Shift>0.033</Row_Peak_Shift>
    <Row_Peak_Shift>0.066</Row_Peak_Shift>
    <Row_Peak_Shift>0.1</Row_Peak_Shift>
    <Row_Peak_Shift>0.133</Row_Peak_Shift>
    <Row_Peak_Shift>0.166</Row_Peak_Shift>
    <Row_Peak_Shift>0.2</Row_Peak_Shift>
    <Row_Peak_Shift>0.233</Row_Peak_Shift>
    <Row_Peak_Shift>0.266</Row_Peak_Shift>
    <Row_Peak_Shift>0.3</Row_Peak_Shift>
    <Row_Peak_Shift>0.333</Row_Peak_Shift>
    <Row_Peak_Shift>0.366</Row_Peak_Shift>
    <Row_Peak_Shift>0.4</Row_Peak_Shift>
    <Row_Peak_Shift>0.433</Row_Peak_Shift>
    <Row_Peak_Shift>0.466</Row_Peak_Shift>
    <Row_Peak_Shift>0.5</Row_Peak_Shift>
</List_of_Row_Peak_Shifts>
```

The input values denote a shift of the peak in the unit of ACCD columns. The default setting in E2S v3.04 describes a shift going in steady steps from 0 columns in the lower most bin to 0.5 columns in the upper most bin. Oliver Reitebuch suggests (based on evidence from the A2D) to change this to 0.21 columns (bottom/top). Then the discretization would be 0.014. This suggestion was received after the test was run; therefore we have kept to the original setting. Presumably the smaller tilt would lead to a smaller effect by a roughly linear amount.

An example of a tilted Mie fringe is taken from [RD3] as shown in Figure 14, this example matches the Mie fringe tilt parameters chosen for the test case.
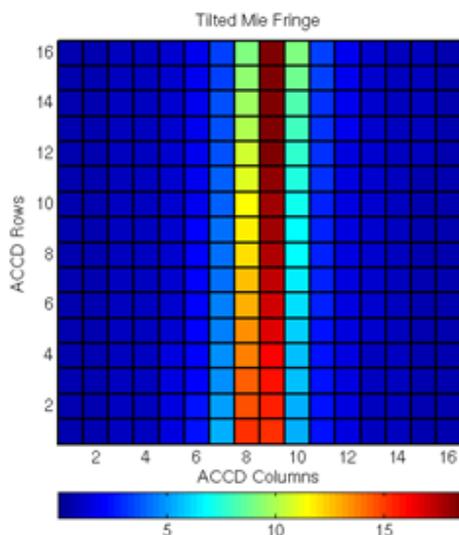
Figure 14. Example of a tilted Mie fringe on the ACCD from [RD3]. This is the same shift as tested here, i.e. no shift at bottom to 0.5 of a column at the top.
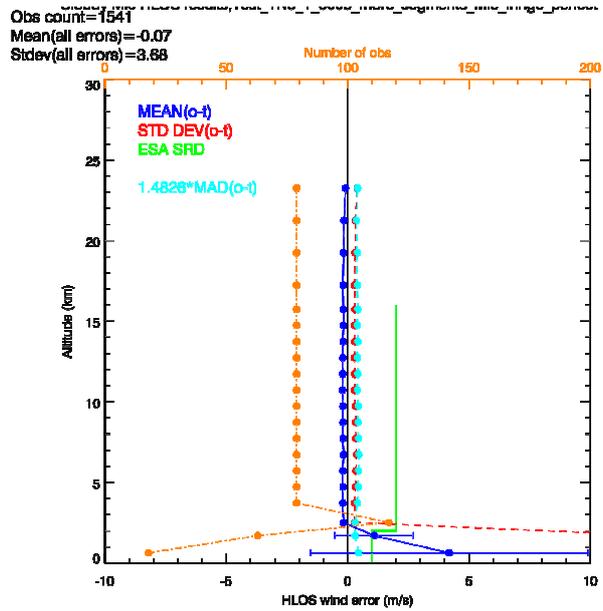
5.1 Test case

It was decided to run a modified version of the test case used in section 2 i.e. the 80 BRC case with wind constant in the vertical but varying regularly horizontally, and with no noise. It is modified by including the aerosol content of the KNMI atmospheric database scene (single_RMA_profile_subarctic_winter). The backscatter coefficient it is multiplied by a factor of 100 to provide many Mie results and hence to allow the assessment of the tilted fringe on the winds. The CoP was run twice, once with the tilted fringe "on" and once with it "off". A more realistic scenario was not run due to time constraints, and also due to the experience with the Rayleigh imperfections (having similar results for realistic and artificial atmospheres). However, in hind sight the more realistic scenario should have been tested, because this effect may interact with vertical wind shear.
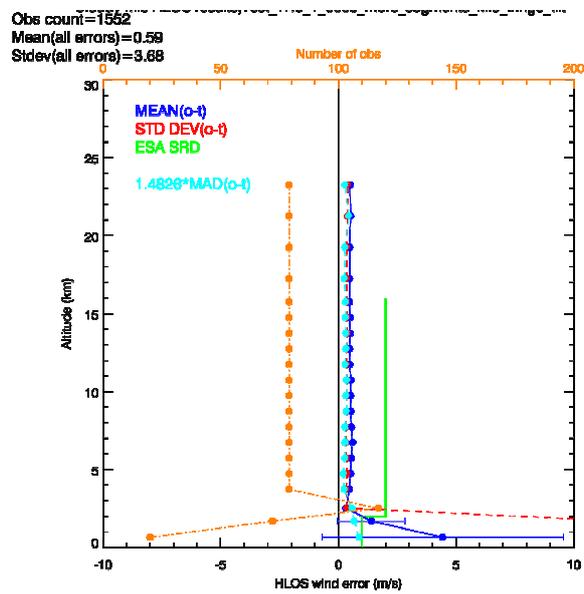
5.2 Results

Figure 15 shows the main results of the tests. It compares the error statistics without the Mie fringe tilt a) to with the tilt in b). It is apparent that the bias (dark blue line) has changed by + 0.66 m/s when including the Mie fringe tilt. This level of bias presumably depends on the size of the tilt of the Mie fringe. Note that the bias is assumed to vary linearly with Mie fringe tilt; hence a tilt of 0.21 as suggested by Oliver may have produced a bias of 0.26 m/s.

A possible explanation for the bias might be that the fringe tilt effectively blurs the knowledge of the Doppler shift across the ACCD (the x position of the fringe peak is supposed to correspond to the Doppler shift). Furthermore, in this test a tilted Mie fringe measurement is used in combination with an MRC assuming no fringe tilt, causing a mismatch between calibration and measurements resulting in the bias. **It's unclear whether the problem would go away if the calibration was also simulated with the same Mie tilt**. One would imagine that the horizontal blurring (in effect) of the Mie fringe function would only degrade the ability to locate the peak position, and hence the sensitivity of the measurement for detecting Doppler shift. Testing with new calibration files with the same imperfections will be done as part of CCN5 WP2810 (L2BP performance with calibration loops).

a)

b)

Figure 15. L2B Mie-clear wind error statistics for a) with no tilt of Mie fringe and b) with a tilt of the Mie fringe.

6 ADAM reflectance map

Instead of using a constant surface reflectance value, the E2S v3.04 allows the user to use maps of surface reflectance which vary globally and change with each month of the year in a much more realistic manner. This will improve the simulation of Aeolus ground returns which are necessary for Zero Wind Calibration. The ADAM (**A** surface reflectance **Da**tabase for ESA's EO **M**issions) surface reflectance maps (which are stored as NetCDF files) were downloaded from the e-room:

`AEOLUS > UPLOAD_ESTEC > ADAM_albedo_map >`

`albedo_maps_ADAM_20140303.tar.gz`

The maps were provided by T. Kanitz at ESA-ESTEC - they are applicable for the Aeolus laser wavelength and measurement viewing geometry (off-nadir pointing). The maps were extracted from the ADAM database (http://adam.noveltis.fr/). ADAM was created by Noveltis and partners under ESA study contract 4000102979, under the supervision of A.G. Straume (ESA-ESTEC). The absolute path to the reflectance maps was put in as a parameter in `*atmosphereGroundParameters.xml` input files for the test scenario. A new flag in the `*atmosphereGroundParameters.xml` allows to select the use of the data in these maps.

6.1 Test case

A new Chain-of-Processors test scenario generated at ECMWF was chosen:

`Test_ECMWF_scene_from_AUX_MET_2011040400_16km`

This is a realistic scenario based on input meteorological fields (i.e. HLOS wind, temperature, pressure, cloud extinction/backscatter) from the ECMWF model at T1279 (~16 km grid size), and sampled with a segment every 16 km (on 4th April 2011) along the ground-track along a realistic Aeolus orbit that can be matched in the E2S. It is just over one orbit long. The cloud backscatter and extinction are forward modelled from the ECMWF cloud liquid/ice water content (using fairly standard parameterisations) - hydrometeors and aerosol optical properties were not considered.

This is a useful scenario to test the quality of the ground return signal since the ECMWF orography matches the E2S due to extracting ECMWF fields along a simulated Aeolus orbit (unlike in the CALIPSO test scenarios where there is a mismatch between CALIPSO orbit and E2S Aeolus orbit). Also the reasonable representation of cloud optical properties (ECMWF model clouds are known to match CALIPSO fairly well) leads to a reasonable simulation of the signal available at the surface, which of course affects the quality of ground return and hence the Zero Wind Correction (ZWC) values.

It should become clear from the ZWC results whether the ADAM reflectance map is correctly implemented i.e. whether good ZWC values are correlated with high reflectances. Also, it's interesting to see how the quality of L1B zero-wind correction (ZWC) values obtained with realistic reflectances compares to a constant surface reflectance. Previous testing has used a constant albedo of 0.8 everywhere, and can hence be used for comparison.

The E2S random noise settings were set to the defaults (i.e. "on"), and there was no bias (i.e. miss-pointing) in the AOCS, therefore the "true" ZWC value should be 0 m/s. Only the L1B processor is needed (i.e. L2B processor not used) for this assessment of the ZWC values (the same values are

passed onto the L2B processor).

Given that the test scenario is in the month of April we expect the E2S to select the reflectance map `BRDF__apr.nc`. Thomas Kanitz (ESA-ESTEC) has produced an image of this reflectance map for the end of April, which is replicated in Figure 16. High reflectances can be found over snow/ice covered areas and over desert regions. Lowest reflectances occur over vegetation.
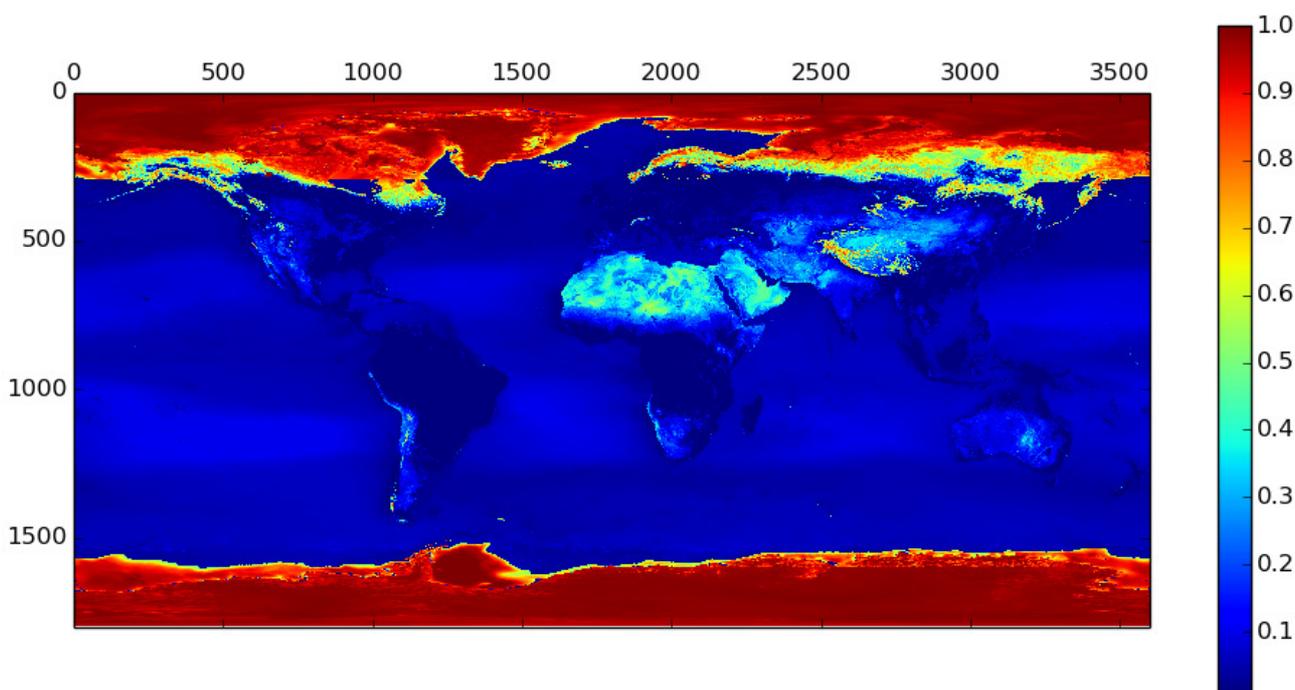

Figure 16. Plot of the map of surface reflectance values for the end of April from ADAM. Image courtesy of T. Kanitz.

The reading of the NetCDF file failed in the E2S when using Matlab v2010a. However, it succeeded with Matlab v2013a, presumably because this newer version can cope with the NetCDF v4 file format.

6.2 Results

Figure 17 shows the L1B processor ZWC values (one per BRC) for the Rayleigh (red) and Mie (green) channels, superimposed on the cross-sectional view of the scattering ratio (SR) (E2S input). The SR information helps to explain the quality of the ZWC values, i.e. the amount of laser light transmitted to the surface and back to the satellite. The ZWC values are extracted from the L1B product. The ZWC value can be read off the values on the height axis in m/s (e.g. 5 km corresponds to 5 m/s) i.e. the ordinate should say "Height (km) or ZWC value (m/s)". This plot only shows the ZWC values that were retrieved, i.e. it does not repeat the last available valid ZWC value (from pervious BRCs); a now obsolete method employed in the L1Bp. Some features noted from the figure:

- The Rayleigh ZWC values (red) are much noisier than the Mie ones (green), showing many retrieved non-zero values.
- ZWC values are missing for both Mie and Rayleigh below optically thick clouds
- The most accurate results correlate well with clear atmospheric conditions

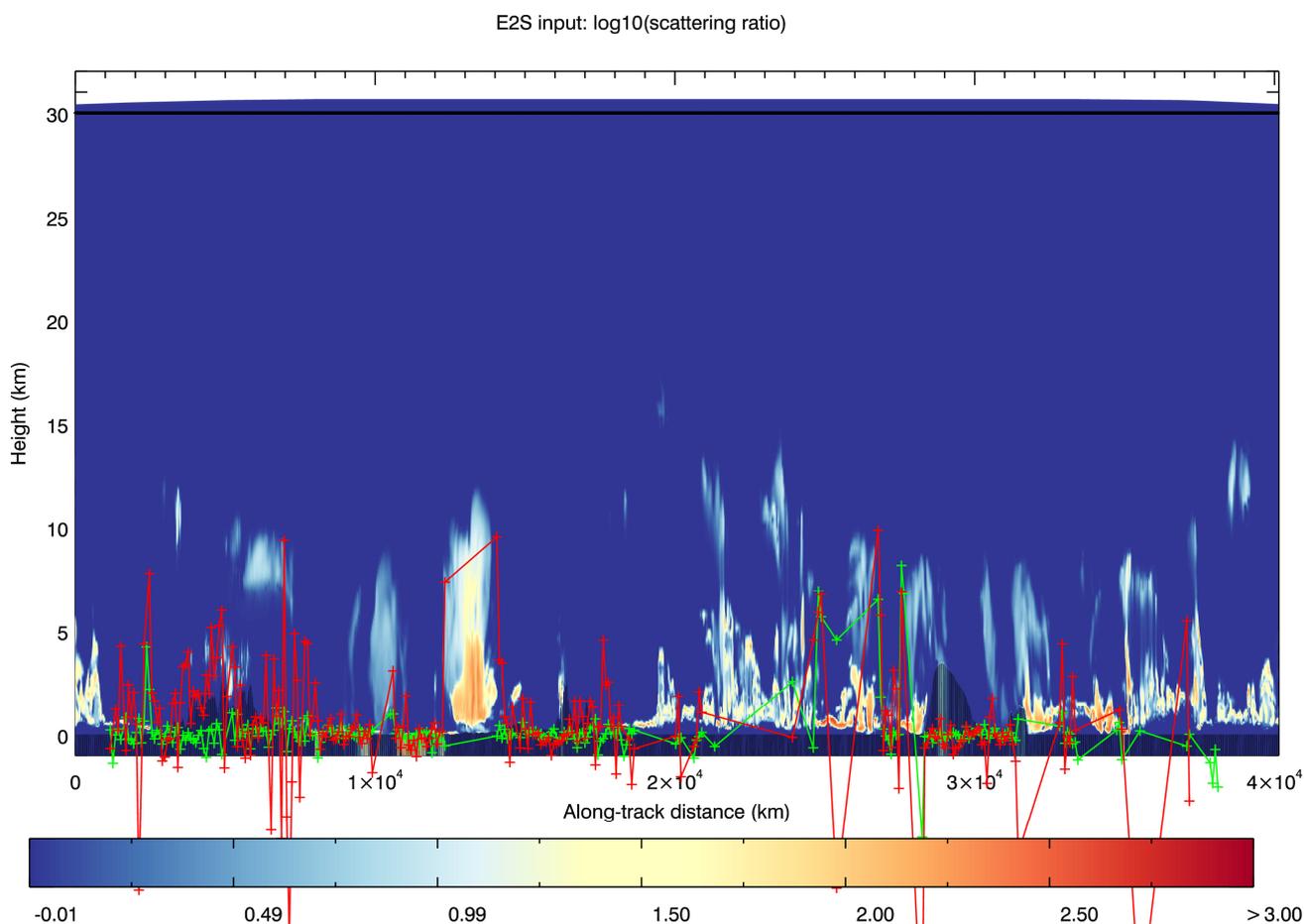- There are stretches over 1000s km with reasonable ZWC values for the Mie

E2S input: log10(scattering ratio)

Figure 17. Cross-section of log$_{10}$(scattering ratio) and ZWC values for Rayleigh (red) and Mie (green) (ordinate axis is either Height (km) for reading scattering ratio, or ZWC value (m/s) for reading the ZWC values).

Figure 18 shows a map of the values of the ZWC for the Rayleigh channel. The Aeolus orbital ground-track is apparent; starting at roughly -100 degrees west (Figure 20 assists in the comparison with Figure 17). The dark blue values are missing values (-9999, less than -12 m/s). Missing values occur when ZWC values were not retrieved for particular BRCs due to lack of a valid ground return signal. Most of the retrieved ZWC values are beige in colour, meaning the values are close to 0 m/s (close to the "truth"). Figure 19 shows the same type of plot for the Mie channel. Some features noted from both figures:

- Most of the good retrievals of Mie ZWC occur over land areas e.g. North America (Rocky Mountains) and Antarctica. This is thanks to a combination of cloud-free or optically thin cloud conditions and higher reflectances (ice/snow over Antarctica and desert/snow over land areas). Over Antarctica, the cloud free or optically thin cloud conditions combined with the high surface reflectance led to very good ZWC results for both the Rayleigh and the Mie (see ~3E4 km along-track distance). Also, good results for both channels are seen over the Arctic.
- The ocean areas tend to be cloudier than land for this example case at least, which limits the number of accurate ZWCs. However, in a few locations where the atmosphere is clear enough

retrievals are possible (e.g. see over the Arabian Sea) but the quality is not the best due to low surface reflectance.

- The general conclusion is that optically thick clouds are the main limiter for getting good Mie channel ZWC retrievals. For example over the Rockies and the Middle East, the Mie ZWCs are of good quality; despite of a moderate surface reflectance (0.2-0.4) i.e. the SNR of the ground return must be sufficient. However the Rayleigh ZWCs over the Rockies look very noisy, implying the surface reflectance is too low to provide enough SNR. Hence, for the Rayleigh it appears that accurate ZWC values are restricted to clear atmosphere and high surface reflectance. This confirms the outcome of earlier investigations done under this contract and the parallel Aeolus L1b processor development contract.

L1B Ray results positions, from file:
from_AUX_MET_2011040400_16km/AE_TEST_ALD_U_N_1B_20110404T011556059_005556000_019937_0001.TXT
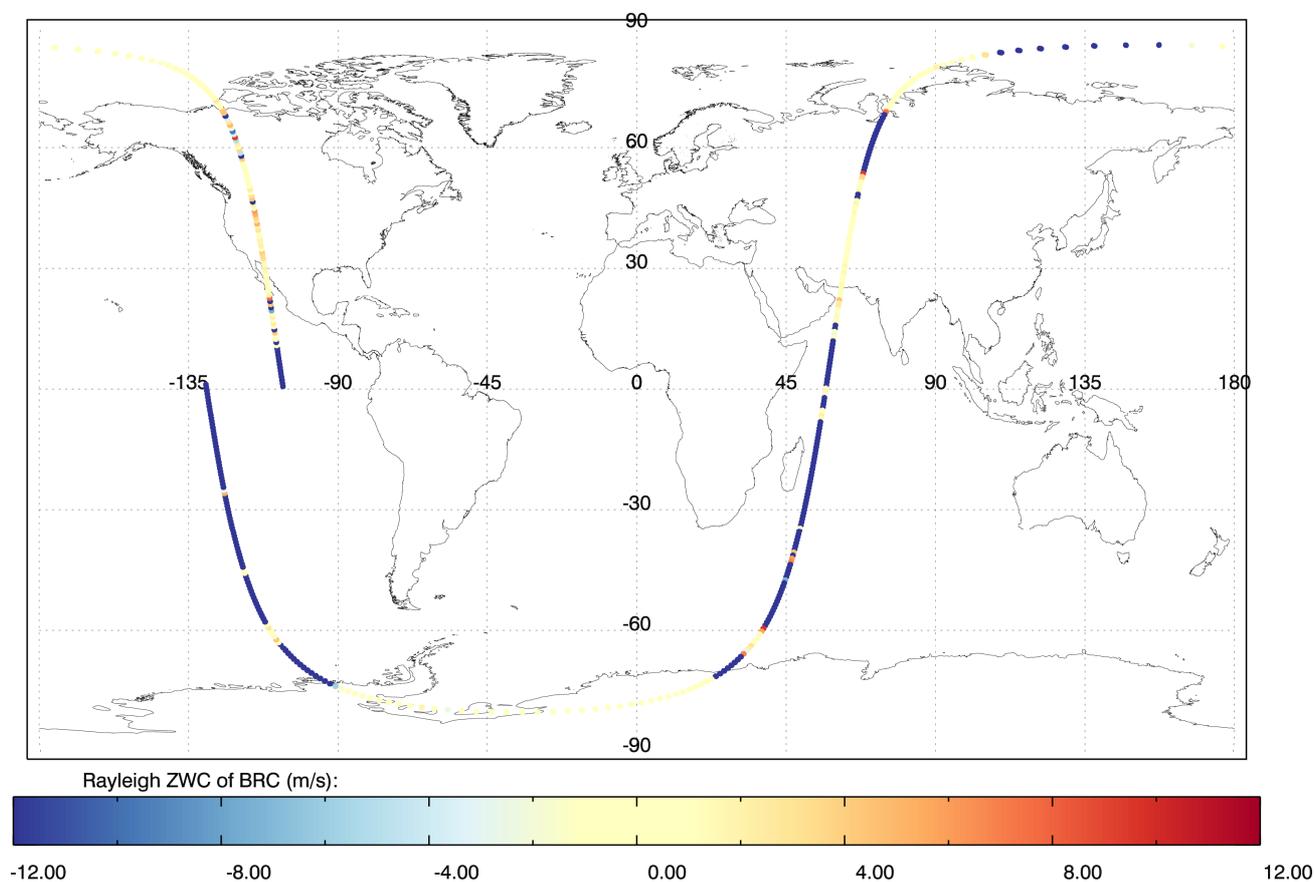

Figure 18. Location on map of ZWC results for the Rayleigh channel. Values less than -12 m/s (dark blue) are missing values.

L1B Mie results positions, from file:
from_AUX_MET_2011040400_16km/AE_TEST_ALD_U_N_1B_20110404T011556059_005556000_019937_0001.TXT
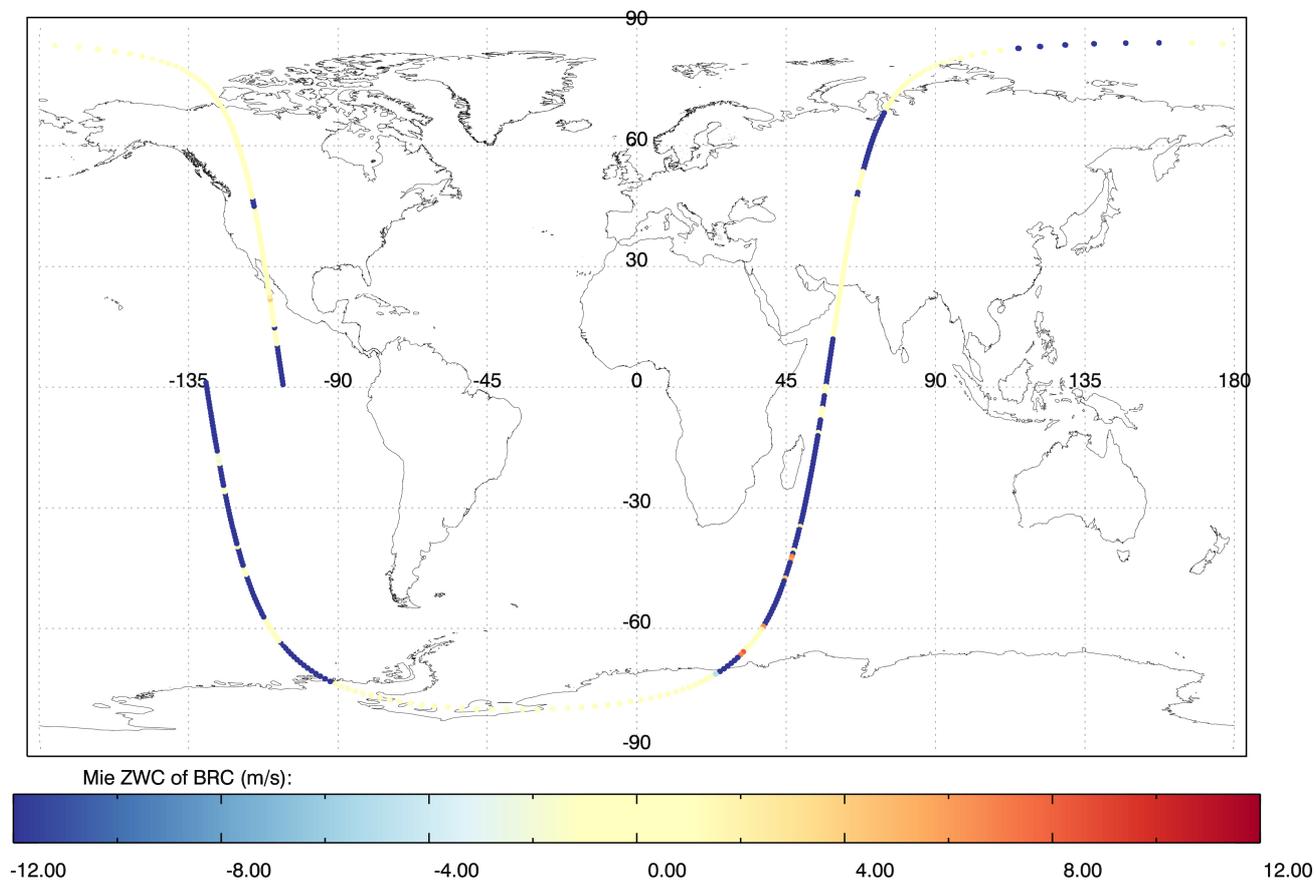

Mie ZWC of BRC (m/s):

Figure 19. Same as Figure 18 but for the Mie ZWC values.

L1B Rayleigh results positions, from file:
from_AUX_MET_2011040400_16km/AE_TEST_ALD_U_N_1B_20110404T011556059_005556000_019937_0001.TXT

Along_track distance of observation COG (km):

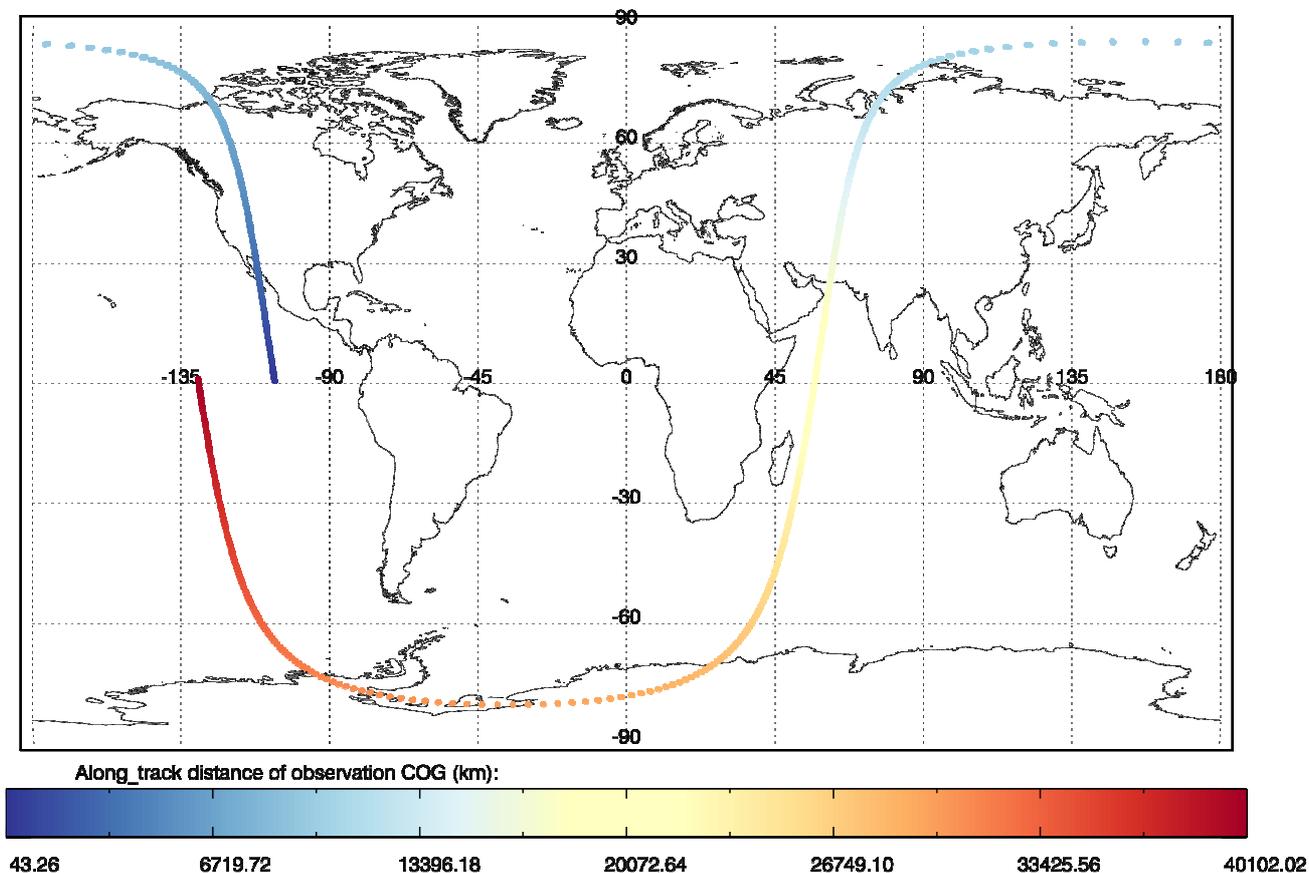| 43.26 | 6719.72 | 13396.18 | 20072.64 | 26749.10 | 33425.56 | 40102.02 |

Figure 20. Along-track distance (km) for the orbit for assistance in comparison of Figure 18 and Figure 19 to Figure 17.

The histograms of Figure 21 and Figure 22 show the distribution of ZWC values relative to the truth (0 m/s) for the Rayleigh and Mie channels respectively. The 1.4826*MAD (Medium absolute deviation) value gives an indication of what the standard deviation of the errors would be if the outliers could be removed (quality control), i.e. a robust statistic. The much larger actual standard deviation indicates that there are many outliers affecting the statistics. Without knowledge of the truth, and with the true zero wind possibly varying with latitude in some periodic way, it will not be trivial to remove such outliers in reality.

The 1.4826*MAD values are around 1.1 m/s for the Rayleigh and 0.3 m/s for the Mie channel. The same statistic was calculated to be 0.5 m/s for the Rayleigh and 0.2 m/s for the Mie a few months ago with a constant surface albedo everywhere of 0.8.. That is, with more realistic surface reflectance, the standard deviation is degraded by 50% for the Mie and by 220% for the Rayleigh. This level of increase in error due to more realistic reflectance is a worry regarding the ability to perform an adequate Harmonic Bias Correction for Aeolus - particularly for the Rayleigh channel. It should be noted here that from earlier studies under this and the parallel L1b contract, it was advised to apply Mie ZWC both to Mie and Rayleigh winds because the Mie ZWC is more accurate. However, as shown in eth A2D Campaign analysis, it is probably necessary to apply the Rayleigh ZWC to Rayleigh wind measurements because the correction is different from the Mie one.

It would be useful to plot ZWC error statistics versus the "true reflectance value" input to E2S, however with the ADAM reflectance map these values are not available in the E2S input *.xml files (the usual method used to get the E2S inputs). They are however stored in the instrumentData directory when converted to *.m (Matlab format), but this would require changing the verification software to accommodate this, and hence has not been done for this study. The L1B team intends to investigate ZWC in much more depth anyway, so I leave it to their study.
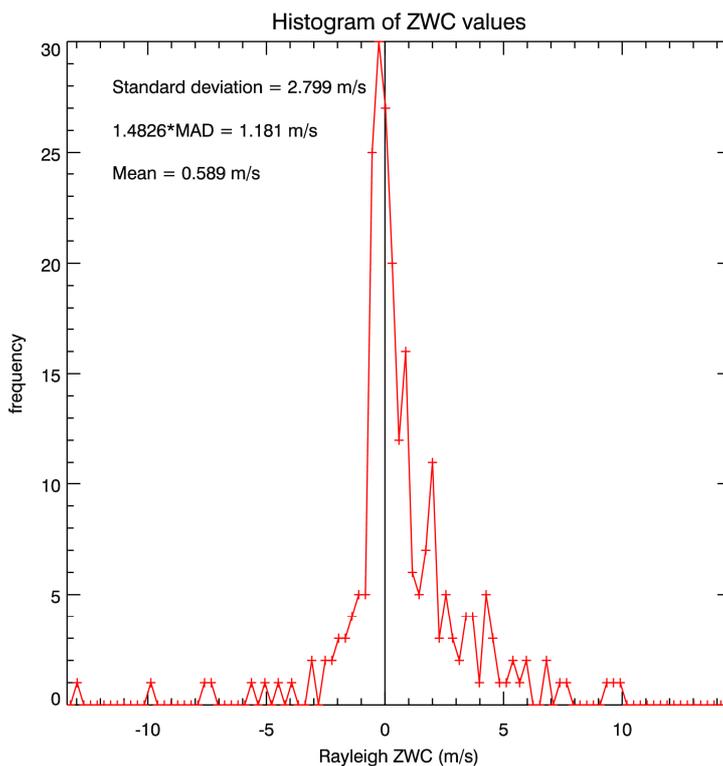

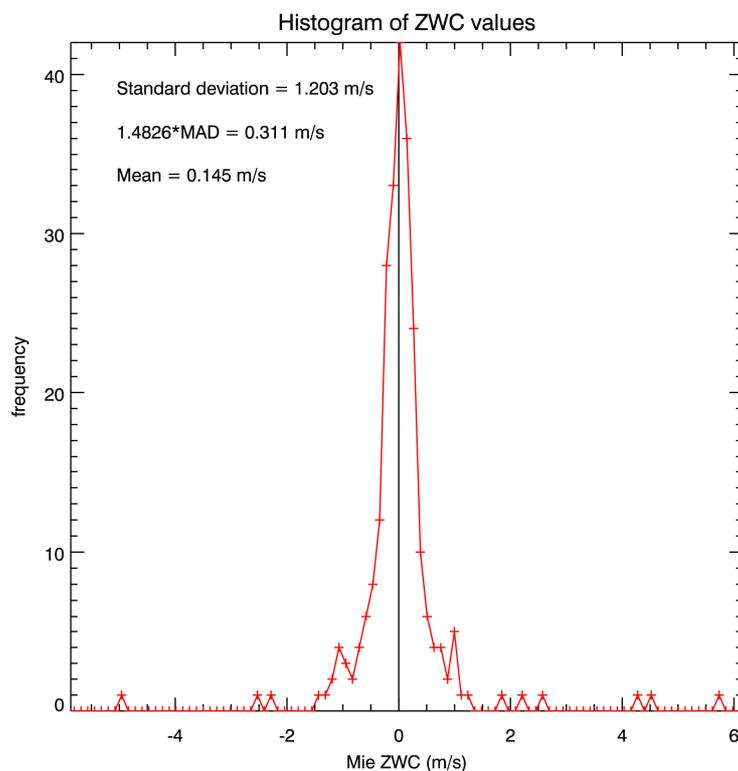**Figure 21. Histogram of Rayleigh ZWC values. The truth is 0 m/s.**

Figure 22. The same Figure 21, but for the Mie channel.

7 Conclusions

In this report, the effect of some new E2S simulation features upon the L2B and ZWC estimates was investigated. The main findings were:

- The RB scattering simulation in E2S can be accurately corrected in the L2Bp when used with the appropriate AUX_RBC_L2 calibration file
- The biases from a lack of pressure and temperature correction in the Rayleigh winds tend to cancel at high pressures for the L1B processing.
- Vertical-bin-overlap alone is not a great issue for the quality of atmospheric winds from Aeolus, but when combined with spectrometer imperfections it can lead to worrying large biases for both the Rayleigh and Mie channels. It is unclear at this stage if calibration with the same imperfections would improve the situation.
- The ZWC correction value quality is significantly impaired when simulated with a realistic surface reflectance map compared to a constant value of 0.8. The random errors are worse by 50% for the Mie and 220% for the Rayleigh. It does not look promising for the Rayleigh channel HBE calibration; however the Mie channel quality still looks good.